Segregation of helicity in inertial wave packets

A. Ranjan*
Department of Engineering, University of Cambridge, Cambridge, United Kingdom
(Received 22 October 2016; published 24 March 2017)

Inertial waves are known to exist in the Earth's rapidly rotating outer core and could be important for the dynamo generation. It is well known that a monochromatic inertial plane wave traveling parallel to the rotation axis (along positive z) has negative helicity while the wave traveling antiparallel (negative z) has positive helicity. Such a helicity segregation, north and south of the equator, is necessary for the α^2-dynamo model based on inertial waves [Davidson, Geophys. J. Int. **198**, 1832 (2014)] to work. The core is likely to contain a myriad of inertial waves of different wave numbers and frequencies. In this study, we investigate whether this characteristic of helicity segregation also holds for an inertial wave packet comprising waves with the same sign of $C_{g,z}$, the z component of group velocity. We first derive the polarization relations for inertial waves and subsequently derive the resultant helicity in wave packets forming as a result of superposition of two or more waves. We find that the helicity segregation does hold for an inertial wave packet unless the wave numbers of the constituent waves are widely separated. In the latter case, regions of opposite color helicity do appear, but the mean helicity retains the expected sign. An illustration of this observation is provided by (a) calculating the resultant helicity for a wave packet formed by superposition of four upward-propagating inertial waves with different wave vectors and (b) conducting the direct numerical simulation of a Gaussian eddy under rapid rotation. Last, the possible effects of other forces such as the viscous dissipation, the Lorentz force, buoyancy stratification, and nonlinearity on helicity are investigated and discussed. The helical structure of the wave packet is likely to remain unaffected by dissipation or the magnetic field, but can be modified by the presence of linearly stable stratification and nonlinearity.

DOI: 10.1103/PhysRevFluids.2.033801

I. INTRODUCTION

In a rapidly rotating system such as the Earth's liquid-iron outer core, the Coriolis force arises to conserve angular momentum in the noninertial frame of reference. Its restoring action results in oscillations which are called inertial waves owing their name to the rotational inertia. Out of the several interesting characteristics of inertial waves that we will discuss in detail later on, two important ones are as follows: (a) inertial waves are helical, i.e., each monochromatic wave has helicity $\boldsymbol{u} \cdot (\boldsymbol{\nabla} \times \boldsymbol{u})$ (which strictly speaking is called helicity density) [1] of one particular sign—either positive or negative; (b) the waves propagating parallel to the axis of rotation possess negative helicity and those traveling antiparallel possess positive helicity [2]. It turns out that this helicity segregation characteristic (negative above and positive below assuming the rotation rate $\boldsymbol{\Omega} = \Omega \boldsymbol{e}_z$) can be successfully used as a diagnostic to detect inertial waves [3,4]. Moreover, it has been proposed recently that inertial waves can even support dynamo action in the Earth's convective outer core (referred to as the core henceforth) and help in sustaining the geomagnetic field against the natural dissipative decay [5]. Obviously, any real or practical medium such as the core will contain several inertial waves, with different frequencies and wave numbers, which will superimpose to form wave packets. It is then natural to ask whether this helicity segregation characteristic of a monochromatic

*ar606@cam.ac.uk

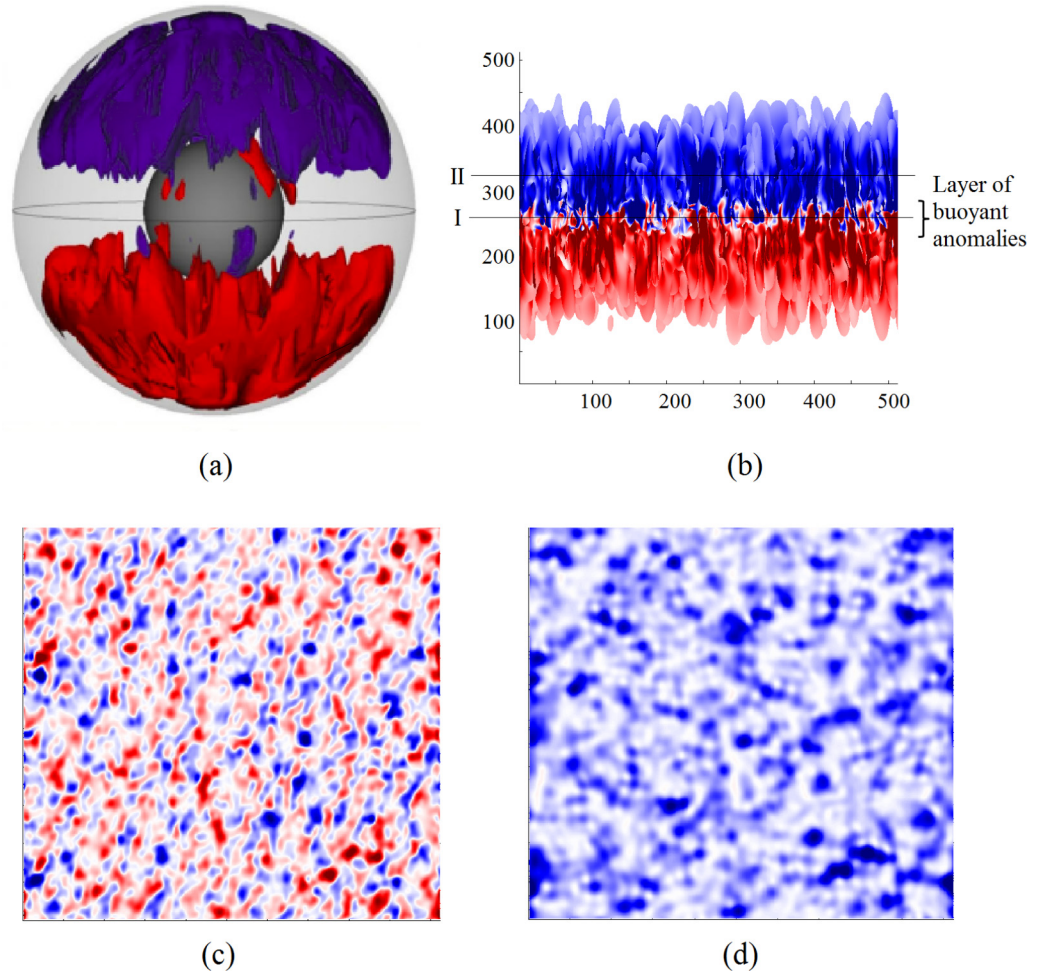

FIG. 1. (a) Helicity isosurfaces in a geodynamo simulation [10], (b) energy isosurfaces colored by helicity above and below a layer of buoyant anomalies [4], and helicity on the horizontal planes (c) I, (d) II shown in (b). Red is positive and blue is negative helicity. Images are obtained with permission from Oxford University Press.

inertial wave also holds for a wave packet always. Indeed, this is *the* central question that we seek to answer in this study.

Helicity, which physically signifies the "writhe and twist" among the streamlines and the vortex lines, is considered to be an important ingredient in the α^2-dynamo model for the core [2,6]. According to this model, the lifting and twisting of magnetic field lines by the flow (hence the role of helicity), can create the poloidal component of the magnetic field from the toroidal (and vice versa) thus sustaining the dynamo [7]. However, this model works only if there is a segregation of helicity north and south of the equator outside the tangent cylinder circumscribing the inner core [8]. This is indeed observed in geodynamo simulations [9,10] [see Fig. 1(a) for example] and leads us to ask if it could be linked to the helicity segregation characteristic of inertial waves. In a seminal study, Moffatt [2] found that a random superposition of inertial waves *can* produce a self-sustaining dynamo in a rotating conducting fluid with nonzero helicity. However, if the waves going upwards and downwards superimpose in equal proportions, then the helicity will obviously be zero. Therefore, the model needs a mechanism to have a preferential distribution of more waves propagating upwards

than downwards in the northern hemisphere in order to create negative helicity (and the other way around in the south). Interestingly, such a mechanism exists in the core in the form of a preferential concentration of buoyant anomalies near the equator, at least in the geodynamo simulations [11], which can act as a localized source of inertial waves. This observation was exploited by Davidson [5] to propose a α^2-dynamo cartoon based on near-zero frequency inertial waves, which was found to work very well in a periodic box with a layer of buoyant anomalies [4] [Fig. 1(b)]. However, this cartoon depends on whether or not the helicity segregation property of a monochromatic inertial wave extends to wave packets, the subject of the present study.

To remind the reader of the helical nature of inertial waves, let us briefly review their well-known theory [12]. For an incompressible fluid, the momentum equation in a rotating reference frame is written as

$$\frac{D\boldsymbol{u}}{Dt} = -\frac{1}{\rho}\boldsymbol{\nabla}\tilde{p} + \nu\frac{\partial^2\boldsymbol{u}}{\partial\boldsymbol{x}^2} - 2\boldsymbol{\Omega}\times\boldsymbol{u}, \tag{1}$$

where $\tilde{p} = p - (\rho/2)(\boldsymbol{\Omega}\times\boldsymbol{x})^2$ incorporating the centrifugal force. If the flow is inviscid and at very low Rossby number, $\mathrm{Ro} = u/2\Omega l$, then

$$\frac{\partial\boldsymbol{u}}{\partial t} = -\frac{1}{\rho}\boldsymbol{\nabla}\tilde{p} - 2\boldsymbol{\Omega}\times\boldsymbol{u}. \tag{2}$$

Taking the curl of (2) and using incompressibility leads to

$$\frac{\partial\boldsymbol{\omega}}{\partial t} = 2(\boldsymbol{\Omega}\cdot\boldsymbol{\nabla})\boldsymbol{u}, \tag{3}$$

where $\boldsymbol{\omega} = \boldsymbol{\nabla}\times\boldsymbol{u}$ is the vorticity. Applying $\boldsymbol{\nabla}\times\partial/\partial t$ to (3), using (2) and $\boldsymbol{\nabla}\cdot\boldsymbol{u} = 0$, leads to

$$\frac{\partial^2}{\partial t^2}(\nabla^2\boldsymbol{u}) + 4(\boldsymbol{\Omega}\cdot\boldsymbol{\nabla})^2\boldsymbol{u} = 0. \tag{4}$$

This equation supports plane waves of the form

$$\boldsymbol{u} = \hat{\boldsymbol{u}}\exp[i(\boldsymbol{k}\cdot\boldsymbol{x} - \varpi t)] \tag{5}$$

and is hyperbolic if $\varpi^2 \leqslant 4\Omega^2$, where $i^2 = -1$. The dispersion relation, therefore, is

$$\varpi = \pm\frac{2(\boldsymbol{k}\cdot\boldsymbol{\Omega})}{k} = \pm\frac{2k_z\Omega}{k}, \tag{6}$$

where $k = |\boldsymbol{k}|$. The group velocity of inertial waves is given by

$$\boldsymbol{C_g} = \pm\frac{2\boldsymbol{k}\times(\boldsymbol{\Omega}\times\boldsymbol{k})}{k^3}. \tag{7}$$

It is interesting to note that the frequency ϖ is independent of the wave number k, but depends on θ, the orientation between $\boldsymbol{\Omega}$ and $\boldsymbol{k}$. This means $\varpi = \pm 2\Omega\cos\theta$ and

$$\boldsymbol{C_g} = \pm\frac{2\Omega}{k}(\hat{\boldsymbol{e}}_\Omega - \cos\theta\hat{\boldsymbol{e}}_k), \tag{8}$$

where $\hat{\boldsymbol{e}}_\Omega$ and $\hat{\boldsymbol{e}}_k$ are unit vectors along $\boldsymbol{\Omega}$ and $\boldsymbol{k}$ respectively. From (5), the vorticity can be written as

$$\boldsymbol{\omega} = i\boldsymbol{k}\times\hat{\boldsymbol{u}}\exp[i(\boldsymbol{k}\cdot\boldsymbol{x} - \varpi t)],$$

so that $\hat{\boldsymbol{\omega}} = i\boldsymbol{k}\times\hat{\boldsymbol{u}}$ is the vorticity amplitude. Using (3) we can write

$$-i\varpi(\boldsymbol{k}\times\hat{\boldsymbol{u}}) = 2(\boldsymbol{k}\cdot\boldsymbol{\Omega})\hat{\boldsymbol{u}}. \tag{9}$$

Furthermore, using the dispersion relation (6),

$$\hat{\boldsymbol{\omega}} = i\boldsymbol{k}\times\hat{\boldsymbol{u}} = \mp k\hat{\boldsymbol{u}}, \tag{10}$$

which means that the vorticity and velocity amplitudes for a monochromatic inertial wave are aligned. The helicity of the wave is maximal with

$$\hat{h} = \mp k|\hat{\boldsymbol{u}}|^2. \tag{11}$$

If the vorticity and velocity were not aligned, then $|\hat{\boldsymbol{u}} \cdot \hat{\boldsymbol{\omega}}| < |\hat{\boldsymbol{u}}||\hat{\boldsymbol{\omega}}|$ and the wave would not be maximally helical. More importantly, this result indicates inertial waves with negative helicity (or positive $\boldsymbol{\Omega} \cdot \boldsymbol{C_g}$) travel upwards, whereas those with positive helicity travel downwards [2] [note that the phase of a vertically propagating wave is $k_z(z \mp 2\Omega t/k)$]. The low-frequency inertial waves, with $\varpi \approx 0$, are particularly important as they travel nearly parallel to the rotation axis with group speed $C_g \approx 2\Omega/k$ [see Eq. (8)], and lead to the formation of columnar vortices [3,4,13].

With their many interesting properties, inertial waves have intrigued scientists, engineers, and mathematicians alike. There is an oft-forgotten but important distinction between the inertial waves in an unbounded domain and those in a confined domain, also called inertial modes [14]. There are several studies on inertial modes in confined rotating systems such as a spherical shell or a cylindrical annulus [15,16]. For example, in a recent study for a rotating annulus, Zhang, Liao, and Kong [16] suggested that inertial modes excited by thermal convection interact nonlinearly to create a transition from laminar to weakly turbulent flow. However, as we shall see later, the inertial modes in a confined domain are not always maximally helical along $\pm z$. Therefore, in this study, we shall restrict our discussion to (unbounded) inertial waves, and in the linear limit of small Ro. Although the presence of a spherical boundary may be important in the core, inertial waves can be triggered by localized sources far from the boundaries, also known as the "far-field approximation" [17]. Examples of such localized sources are the buoyant anomalies near the equator [11] that can radiate low-frequency inertial waves and help maintain the columnar flow in the core, an important ingredient in maintaining a dipolar magnetic field [9].

In a geophysical or astrophysical setting, along with the Coriolis force, there exist several others, such as the Lorentz force due to the coupling of the magnetic field with the velocity, the force due to buoyancy stratification and the dissipative force, all or some of which could be important. Thus arises a curiosity to find out if these forces could influence the helical structure of inertial wave packets. Towards the end of the paper, we will briefly discuss this point in light of the present study and earlier research. But first, we shall derive a general form of the polarization relations for inertial waves (Sec. II). Using these relations, we shall subsequently evaluate the helicity of a wave packet forming as a result of linear superposition of inertial waves (Sec. III). As an illustration, in Sec. IV, we shall compute the helicity for a Gaussian eddy under rotation using direct numerical simulation (DNS) in a periodic box at Ro = 0.09.

II. POLARIZATION RELATIONS

In this section, we derive the relationships between the individual velocity component amplitudes, also called the polarization relations. The equation of motion (1) can be written in Fourier space as

$$(-i\varpi + \nu k^2)\hat{u}_i + ik_j\hat{u}_j\hat{u}_i = -ik_i\hat{p} + 2\epsilon_{ijm}\hat{u}_j\Omega_m, \tag{12}$$

where ϵ_{ijm} is the Levi-Civita symbol and equals 1 or -1 depending on whether the order of i, j, and m is cyclic or acyclic, respectively, and 0 otherwise. Similarly, the continuity equation in Fourier space is

$$k_i\hat{u}_i = 0. \tag{13}$$

Using (13), ignoring nonlinearity (low Ro) and assuming negligible viscosity, we get

$$-\varpi\hat{u}_i + k_i\hat{p} + 2i\epsilon_{ijm}\hat{u}_j\Omega_m = 0 \tag{14}$$

if we multiply by $-i$. Multiplying it further by k_i and Ω_i, and using (13) we get

$$k^2\hat{p} + 2i\epsilon_{ijm}k_i\hat{u}_j\Omega_m = 0, \tag{15}$$

$$-\varpi u_i\Omega_i + \hat{p}k_i\Omega_i = 0, \tag{16}$$

respectively. With rotation parallel to vertical, i.e., $\boldsymbol{\Omega} = (0,0,\Omega)$, these become

$$k^2\hat{p} + 2i(k_x\hat{u}_y\Omega - k_y\hat{u}_x\Omega) = 0, \tag{17}$$

$$-\varpi\,\hat{u}_z + k_z\hat{p} = 0. \tag{18}$$

[Note that Chandrasekhar [18] had derived the polarization relations assuming $\boldsymbol{k} = (0,0,k)$. Of course, there is no loss of generality if a coordinate axis is assumed to be along the wave vector *for a monochromatic wave*. Our assumption $\boldsymbol{k} = (k_x,k_y,k_z)$ is more general and will be useful in the next section where we will consider a wave packet.] Eliminating $\hat{p}$, and using (13) we can get

$$\begin{aligned}\frac{\hat{u}_x}{\hat{u}_z} &= -\frac{-k^2k_y\varpi + 2i\Omega k_z^2k_x}{2i\Omega k_z\left(k_x^2+k_y^2\right)},\\ \frac{\hat{u}_y}{\hat{u}_z} &= -\frac{k^2k_yk_x\varpi + 2i\Omega k_z^2k_y^2}{2i\Omega k_zk_y\left(k_x^2+k_y^2\right)}.\end{aligned} \tag{19}$$

Using the dispersion relation for inertial waves, which is $\varpi = \pm 2\Omega k_z/k$,

$$\begin{aligned}\frac{\hat{u}_x}{\hat{u}_z} &= \frac{\pm k_yk - ik_xk_z}{i\left(k_x^2+k_y^2\right)},\\ \frac{\hat{u}_y}{\hat{u}_z} &= \frac{\mp k_xk - ik_yk_z}{i\left(k_x^2+k_y^2\right)}.\end{aligned} \tag{20}$$

Therefore,

$$\frac{\hat{u}_x}{\hat{u}_y} = \frac{\pm k_yk - ik_xk_z}{\mp k_xk - ik_yk_z}. \tag{21}$$

In a complex representation, the polarization relations can be written as

$$\begin{aligned}\frac{\hat{u}_x}{\hat{u}_z} &= -\frac{k_xk_z}{k_x^2+k_y^2} \mp i\frac{k_yk}{k_x^2+k_y^2},\\ \frac{\hat{u}_y}{\hat{u}_z} &= -\frac{k_yk_z}{k_x^2+k_y^2} \pm i\frac{k_xk}{k_x^2+k_y^2},\\ \frac{\hat{u}_x}{\hat{u}_y} &= -\frac{k_xk_y}{k_x^2+k_z^2} \pm i\frac{k_zk}{k_x^2+k_z^2},\end{aligned} \tag{22}$$

so that their magnitudes are

$$\left|\frac{\hat{u}_x}{\hat{u}_z}\right|^2 = \frac{k_z^2+k_y^2}{k_x^2+k_y^2}, \quad \left|\frac{\hat{u}_y}{\hat{u}_z}\right|^2 = \frac{k_z^2+k_x^2}{k_x^2+k_y^2}, \quad \left|\frac{\hat{u}_x}{\hat{u}_y}\right|^2 = \frac{k_z^2+k_y^2}{k_x^2+k_z^2}. \tag{23}$$

The velocity amplitude can, therefore, be written in terms of component amplitudes as

$$\begin{aligned}|\hat{u}|^2 = \hat{u}_x^2+\hat{u}_y^2+\hat{u}_z^2 &= \left\{\frac{k_x^2k_z^2+k_y^2k^2+k_y^2k_z^2+k_x^2k^2}{\left(k_x^2+k_y^2\right)^2}+1\right\}\hat{u}_z^2,\\ &= 2\frac{k^2}{k_x^2+k_y^2}\hat{u}_z^2.\end{aligned} \tag{24}$$

As we will soon find out in Sec. III, Eq. (24) is very useful as it helps relate $|\hat{u}|$ with $\hat{u}_z$. If the angle between $\boldsymbol{k}$ and $\boldsymbol{\Omega}$ is θ, and if $(k_x,k_y,k_z) = (k\sin\theta,0,k\cos\theta)$, the equations become

$$\hat{u}_z = -\tan\theta\hat{u}_x, \quad \hat{u}_z = \mp i\sin\theta\hat{u}_y, \quad \hat{u}_x = \pm i\cos\theta\hat{u}_y. \tag{25}$$

(i) If $\theta = 0$, the amplitudes $\hat{\boldsymbol{u}} = \hat{u}_x(1, \pm i, 0)$.
(ii) If $\theta = \pi/2$, the amplitudes $\hat{\boldsymbol{u}} = \hat{u}_z(0, \mp i, 1)$.

Under these conditions, inertial waves are circularly polarized, i.e., the velocity field rotates with a constant amplitude in a direction perpendicular to the rotation axis. As a validation, using the polarization relations (22), we can derive the vorticity amplitudes using

$$[\hat{\omega}_x, \hat{\omega}_y, \hat{\omega}_z] = [i(k_y\hat{u}_z - k_z\hat{u}_y), i(k_z\hat{u}_x - k_x\hat{u}_z), i(k_x\hat{u}_y - k_y\hat{u}_x)] \tag{26}$$

and we find that we once again arrive at (10), i.e., $\hat{\boldsymbol{\omega}} = \mp k\hat{\boldsymbol{u}}$.

III. LINEAR SUPERPOSITION OF INERTIAL WAVES AND THE RESULTANT HELICITY

In this section, we consider the superposition of inertial wave modes and the resultant sign of helicity. To start with, let us consider the most general form of two inertial waves with the wave-number vectors $\boldsymbol{k}_n = (k_{n;x}, k_{n;y}, k_{n;z})$, and velocities given by $\boldsymbol{u}_n = \hat{\boldsymbol{u}}_n \exp(i\varphi_n)$, where $n = 1, 2$ for the first and the second wave respectively and $\varphi_n = (\boldsymbol{k}_n \cdot \boldsymbol{x} - \varpi_n t)$ are their phases. The amplitude $\hat{\boldsymbol{u}}_n = \sum \hat{u}_{(n;\mathrm{x})}\hat{\boldsymbol{e}}_{\boldsymbol{x}}$, so that the complex component amplitudes $\hat{u}_{(n;\mathrm{x})} = \hat{u}_{[n;(x,y,z)]}$ are related by the polarization relations derived earlier (22). Similarly, the vorticity can be written as $\boldsymbol{\omega}_n = \hat{\boldsymbol{\omega}}_n \exp(i\varphi_n)$, so that the amplitudes for inertial waves are $\hat{\boldsymbol{\omega}}_n = \mp k\hat{\boldsymbol{u}}_n$ (10). Considering at first the contribution from only the x components of the velocity and vorticity to the helicity, i.e., $h_x = \mathrm{Re}[u_x]\mathrm{Re}[\omega_x]$,

$$h_x = \mathrm{Re}[\hat{u}_{1;x}\exp(i\varphi_1) + \hat{u}_{2;x}\exp(i\varphi_2)]\mathrm{Re}[\mp k_1\hat{u}_{1;x}\exp(i\varphi_1) \mp k_2\hat{u}_{2;x}\exp(i\varphi_2)]. \tag{27}$$

If $\hat{u}_{1;(x,r)}$ and $\hat{u}_{1;(x,i)}$ are the real and imaginary parts of $\hat{u}_{1;x}$ respectively (and similarly for $\hat{u}_{2;x}$), then rearranging the above terms after a little algebra, we can write

$$\begin{aligned} h_x = {} & \mp k_1(\hat{u}_{1;(x,r)}\cos\varphi_1 - \hat{u}_{1;(x,i)}\sin\varphi_1)^2 \mp k_2(\hat{u}_{2;(x,r)}\cos\varphi_2 - \hat{u}_{2;(x,i)}\sin\varphi_2)^2 \\ & \mp (k_1 + k_2)[\hat{u}_{1;(x,r)}\hat{u}_{2;(x,r)}\cos\varphi_1\cos\varphi_2 + \hat{u}_{1;(x,i)}\hat{u}_{2;(x,i)}\sin\varphi_1\sin\varphi_2 \\ & - \hat{u}_{1;(x,r)}\hat{u}_{2;(x,i)}\cos\varphi_1\sin\varphi_2 - \hat{u}_{1;(x,i)}\hat{u}_{2;(x,r)}\sin\varphi_1\cos\varphi_2], \end{aligned} \tag{28}$$

which, put simply, is

$$h_x = \mp k_1\mathrm{Re}[u_{1;x}]^2 \mp k_2\mathrm{Re}[u_{2;x}]^2 \mp (k_1 + k_2)\mathrm{Re}[u_{1;x}]\mathrm{Re}[u_{2;x}]. \tag{29}$$

It may be noted that the first term, a perfect square, results from the first wave and hence the helicity is of a particular sign, as expected. However, with two waves superimposed, the net helicity depends on the sign of the third term corresponding to the cross multiplication of amplitudes. To further investigate this, the above expression can be modified as

$$h_x = \mp\frac{k_1 + k_2}{2}(\mathrm{Re}[u_{1;x}] + \mathrm{Re}[u_{2;x}])^2 \mp \frac{k_1 - k_2}{2}(\mathrm{Re}[u_{1;x}])^2 \pm \frac{k_1 - k_2}{2}(\mathrm{Re}[u_{2;x}])^2. \tag{30}$$

It is now evident that either of the last two terms can contribute to an opposite sign helicity depending on whether $k_1 < k_2$ or otherwise. Repeating the procedure to obtain (28) for other velocity and vorticity components, the total helicity can be expressed as

$$h = \mp\left(\sum_{\mathrm{x}=x,y,z} k_1(\mathrm{Re}[u_{1;\mathrm{x}}])^2 + k_2(\mathrm{Re}[u_{2;\mathrm{x}}])^2\right) \mp (k_1 + k_2)\left(\sum_{\mathrm{x}=x,y,z}\mathrm{Re}[u_{1;\mathrm{x}}]\mathrm{Re}[u_{2;\mathrm{x}}]\right). \tag{31}$$

Since the terms due to the cross multiplication of amplitudes occur in pairs, a general expression for the helicity due to the superposition of n inertial waves can be written as

$$h = \mp\left(\sum_{n}\sum_{\mathrm{x}=x,y,z} k_n(\mathrm{Re}[u_{n;\mathrm{x}}])^2\right) \mp \left[\sum_{i,j=1,\ldots,n}^{i\neq j}(k_i + k_j)\left(\sum_{\mathrm{x}=x,y,z}\mathrm{Re}[u_{i;\mathrm{x}}]\mathrm{Re}[u_{j;\mathrm{x}}]\right)\right]. \tag{32}$$

For example, let us now compute the total helicity due to the superposition of four waves propagating along $+z$ assuming the same vertical velocity amplitudes $u_{i;(z,r)} = 0.1$ and $u_{i;(z,i)} = 0.01$. The x, y

TABLE I. Various wave vector combinations superimposed for the helicity field in Figure 2.

Case	Wave vector (k_x,k_y,k_z) combinations[a]	Mean h
A	(1,−1,1), (1,−1,1), (−1,15,1), (−1,1,1)	−0.27
B	(15,−1,1), (1,−1,1), (−1,15,1), (−1,1,1)	−0.35
C	(15,−1,1), (1,−15,1), (−1,15,1), (−1,1,1)	−0.45
D	(15,−1,1), (1,−15,1), (−1,15,1), (−15,1,1)	−0.52

[a]The $C_{g,z}$, calculated using Eq. (7), comes out to be $4\Omega/3\sqrt{3} \approx 0.77\Omega$ for the wave vectors with $k = \sqrt{3}$, and $452\Omega/(227)^{3/2} \approx 0.13\Omega$ for those with $k = \sqrt{227}$.

amplitudes of velocity can be calculated from the polarization relations (22). Four wave vector combinations (A–D) each comprising four waves with the same sign of $C_{g,z}$, listed in Table I, are considered for illustration. We find that for all combinations, the helicity is primarily negative evident from Figs. 2(a)–2(d). However, for the first two combinations (A, B) shown in Figs. 2(a) and 2(b), for

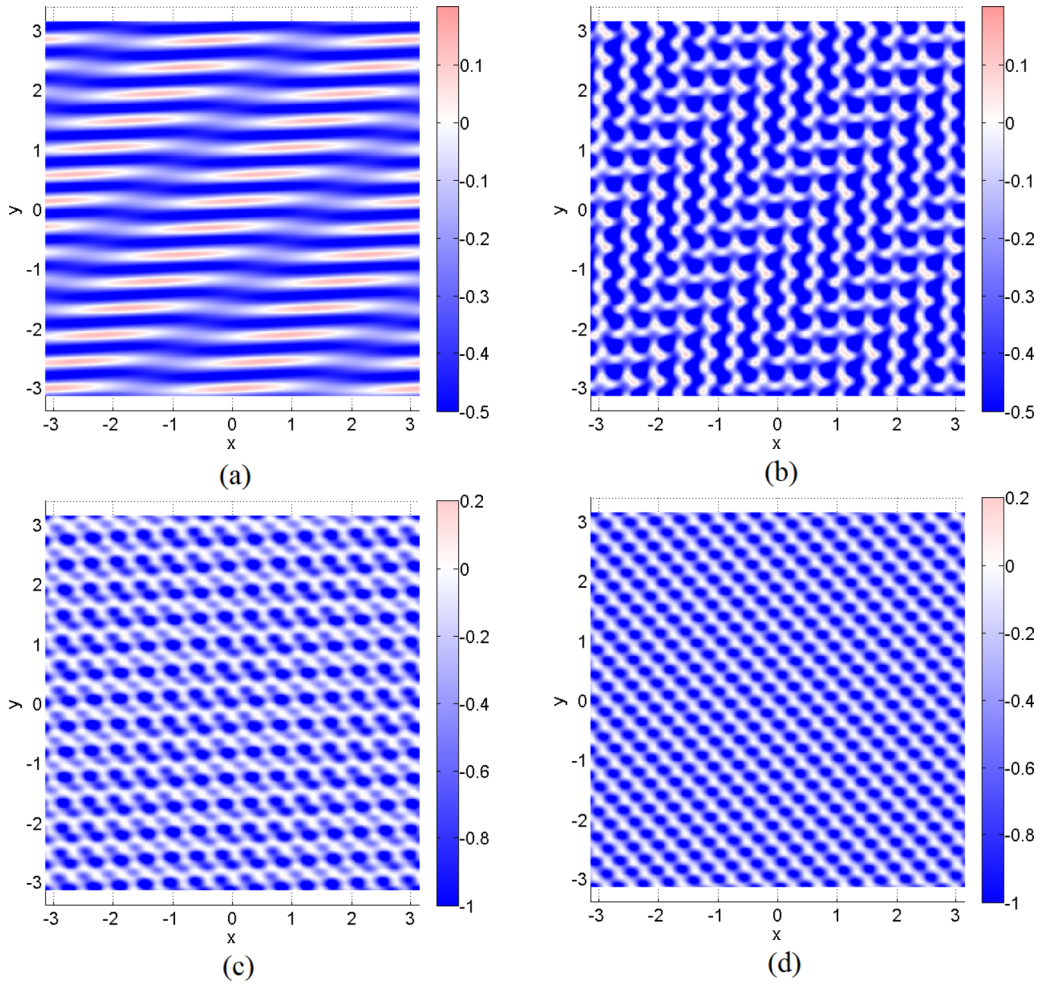

FIG. 2. Helicity h in a horizontal (XY) plane as a result of superposition of four inertial waves at $z = \pi/4$ with wave-vector combinations (a) A, (b) B, (c) C, and (d) D listed in Table I. If we take Ro $= 0.1$ and $l = \pi/k$, we can find $\varpi = k_z\hat{u}/0.1\pi$ if Ro $= \hat{u}/(2l\Omega)$ and $\varpi = 2\Omega k_z/k$. Note the contour threshold is different for the combination A-B to highlight the opposite helicity color.

which $\boldsymbol{k}_i$ is (1,−1,1),(1,−1,1),(−1,15,1),(−1,1,1), and (15,−1,1),(1,−1,1),(−1,15,1),(−1,1,1) respectively, there are periodic regions of opposite sign (i.e., positive) helicity albeit with much lower magnitude. These regions disappear if the wave-number magnitude k_i is the same or nearly the same for all four modes as is evident from Figs. 2(c) and 2(d). Thus, regions of opposite helicity may result if wave modes with a large difference in their wave-number magnitudes are superimposed. Moreover, as a quantitative evidence in support of the above observation, the values of mean helicity listed in Table I show that the magnitude increases from 0.27 for the combination A to 0.52 for D.

For the combinations, if we assume different wave amplitudes, the net effect is to increase or decrease the helicity magnitude without affecting the pattern. Moreover, a phase difference between the superimposed waves alters the locations of the positive and negative helicity but the pattern and the magnitudes remain the same. If waves are superimposed such that some are propagating upwards (positive $C_{g,z}$, negative helicity) and some downwards (negative $C_{g,z}$, positive helicity) then, obviously, helicities of both signs will result. Then, if the wave amplitudes are comparable and there are equal number of upward-propagating and downward-propagating waves, the mean helicity will be close to zero. An example of this situation is homogeneous turbulence in a periodic box under rapid rotation, which will remain nonhelical even though inertial waves may exist locally [19]. The example with four upward-propagating waves considered above is relevant in nonhomogeneous situations, for example in the case of a localized layer of turbulence or buoyancy radiating inertial waves [3,4].

IV. HELICITY OF A GAUSSIAN EDDY UNDER ROTATION

In order to test the results in Secs. II and III, we conduct the DNS of a Gaussian eddy under rapid rotation at Ro = 0.09. The pseudospectral DNS code [20] used for our purpose solves the full governing equations (1) with very low viscosity (initial Re = 26 400 based on the mean velocity and eddy diameter). The time advancement is carried out using the second-order Runge-Kutta (predictor-corrector) scheme, and the viscous terms are evaluated exactly using an integrating factor [21] which is modified to include the rotation [20]. The initial condition is the Gaussian eddy

$$\boldsymbol{u} = \boldsymbol{\Lambda} \times \boldsymbol{x} \exp\left(-\frac{|\boldsymbol{x}|^2}{\delta^2}\right), \tag{33}$$

at the center of a 512^3 periodic box, where δ is the characteristic size, and Λ is the characteristic angular rotation rate of the eddy. The temporal evolution of the eddy is shown in Fig. 3. The first and second rows show the XZ planes for the velocity components u_y and u_z respectively, while the last row shows the helicity. It is evident that the eddy transforms into inertial wave packets which travel along $\pm z$. Moreover, the dominant radiation is parallel to z as expected from theory [13], although there is significant off-axis radiation as well. From the plots of u_y, it is evident that the radiation pattern is in the form of alternating cyclones and anticyclones, with the innermost lobes belonging to the cyclone. (A cyclone has the same sense of rotation as the background, whereas an anticyclone has the opposite.) More importantly, as evident from the last row in Fig. 3, the helicity segregation is in accordance with our predictions in Sec. III, also showing that both cyclones and anticyclones have negative helicity above and positive below. If each lobe is thought of as a slowly modulated wave packet, in which the wave number varies around a peak k_0, the helicity will be primarily of one sign as the difference in wave numbers of the constituent monochromatic waves is likely to be small.

To test the result (24) derived from polarization relations in Sec. II, we plot u^2/u_z^2 at $\Omega t = 8$ in Fig. 4. In the case of a monochromatic wave, this ratio is expected to be equal to $2k^2/(k_x^2 + k_y^2)$. For the vertically propagating waves, $k^2 \approx k_x^2 + k_y^2$ since $k_z \approx 0$, which means the ratio is expected to be $\approx$2. Interestingly, this is also the ratio seen in Fig. 4 indicating that the relationship (24) approximately holds even for wave packets, which is somewhat surprising given that the constituent

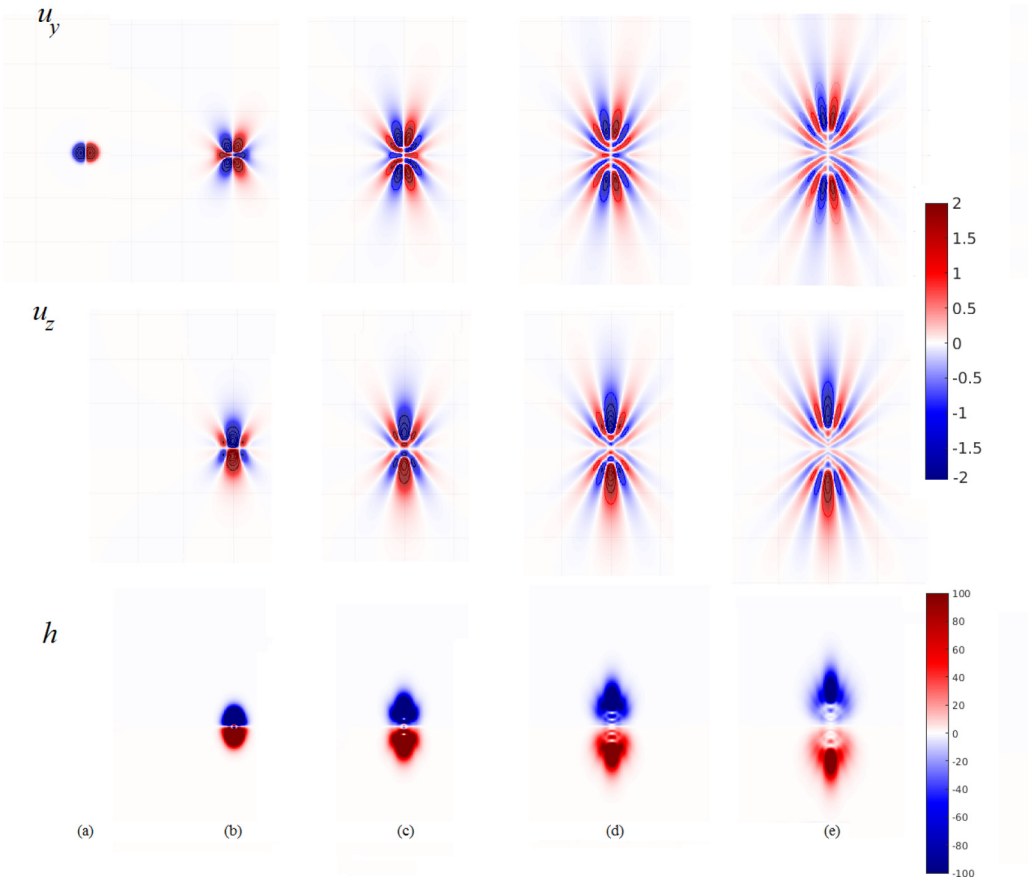

FIG. 3. A Gaussian eddy under rotation for Ωt = (a) 0, (b) 2, (c) 4, (d) 6, (e) 8. The top, middle, and bottom rows show the XZ planes of u_y, u_z, and helicity, respectively. $\delta = 0.125, \Lambda = 300$.

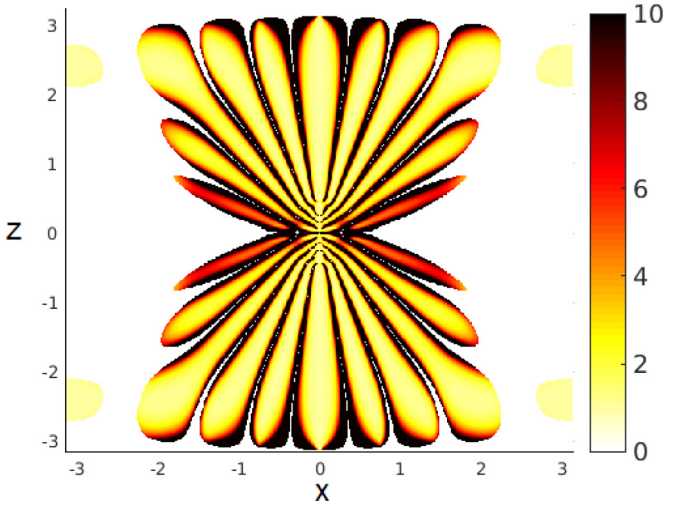

FIG. 4. Plot of u^2/u_z^2 at $\Omega t = 8$. Most regions with $u_z^2 \approx 0$ have been filtered out but some remain and lead to the dark edges around the lobes.

waves can have different amplitudes and phases. Moreover, this ratio is also ~ 2 for the off-axis wave packets with a large $C_{g,z}$ but much larger for other off-axis waves.

V. DISCUSSION

Having found that the helicity segregation characteristic of a monochromatic wave holds for inertial wave packets, we now turn to the effect of the various forces and physical boundaries on their helical structure. Note that each of these effects merits a stand-alone investigation, and has inspired several expositions [8,12,22,23]. For example, Tilgner [23] investigated the effect of stratification and magnetic field on the inertial wave packets radiating from localized sources and found that the magnetic field does not affect the orientation of the wave packets relative to the rotation axis whereas stratification does. However, here we focus specifically on their helical structure and the segregation characteristic.

A. Effect of other forces on helicity

1. Viscous dissipation

The effect of viscosity is to damp the inertial waves but the helical structure remains unchanged. This follows easily if the viscosity of the fluid is included in the governing equations. The resulting vorticity equation is written as

$$\frac{\partial \boldsymbol{\omega}}{\partial t} = 2(\boldsymbol{\Omega}\cdot\nabla)\boldsymbol{u} + \nu\nabla^2\boldsymbol{\omega}, \tag{34}$$

which in turn can be used to write

$$-i(\varpi + i\nu k^2)(\boldsymbol{k}\times\hat{\boldsymbol{u}}) = 2(\boldsymbol{k}\cdot\boldsymbol{\Omega})\hat{\boldsymbol{u}} \tag{35}$$

in Fourier space indicating that velocity and vorticity are still aligned. The modified dispersion relation is

$$\varpi = \pm\frac{2(\boldsymbol{k}\cdot\boldsymbol{\Omega})}{k} - i\nu k^2, \tag{36}$$

which was obtained by Moffatt [8] for a monochromatic wave. Interestingly, the damping does not affect the polarization relations between wave amplitudes. To see how this holds, if the procedure in Sec. II is repeated with viscosity included, we get Eqs. (19) but with $(\varpi + i\nu k^2)$ instead of ϖ. Moreover, using the modified dispersion relation (36), we can also obtain Eqs. (20) once again. In other words, the damped waves can be written in the form $\boldsymbol{u} = \{\hat{\boldsymbol{u}}\exp[i(\boldsymbol{k}\cdot\boldsymbol{x} - \varpi t)]\}\exp(-\nu k^2 t)$. It may be noted that the short-wavelength waves are damped the most with $(\nu k^2)^{-1}$ as the damping time scale. For a damped wave packet, if the procedure in Sec. III is repeated with the damping term included, it is easy to see that the three terms in Eq. (31) will occur multiplied with "$\exp[-\nu(k_i^2 + k_j^2)t]$," where $(i,j) = [(1,1);(2,2);(1,2)]$ for the first, second, and third terms respectively. Clearly, this is unlikely to affect the helicity sign for a wave packet.

2. Lorentz force

If rotation exists in an electrically conducting fluid, then it is natural to ask whether the helicity of inertial waves is modified by the Lorentz force. First Lehnert [24] and later Moffatt [8] observed that the linearized governing equations

$$\frac{\partial \boldsymbol{u}}{\partial t} = -\frac{1}{\rho}\nabla\tilde{p} - 2\boldsymbol{\Omega}\times\boldsymbol{u} + \frac{1}{\rho\mu}(\boldsymbol{B}\cdot\nabla)\boldsymbol{b}, \tag{37}$$

$$\frac{\partial \boldsymbol{b}}{\partial t} = (\boldsymbol{B}\cdot\nabla)\boldsymbol{u}, \tag{38}$$

which include the Lorentz force, support two classes of waves: fast inertial waves whose frequency is mildly modified by the magnetic field and slow magnetostrophic waves. It is interesting to note that both types of waves are helical as their vorticity and velocity amplitudes are aligned,

$$\left(\varpi - \frac{(\boldsymbol{B}\cdot\boldsymbol{k})^2}{\varpi\rho\mu}\right)\hat{\boldsymbol{\omega}} = -(2\boldsymbol{\Omega}\cdot\boldsymbol{k})\hat{\boldsymbol{u}}, \tag{39}$$

where $\boldsymbol{B}$ is the mean magnetic field with $\boldsymbol{b}$ as the fluctuating part, μ is the magnetic permeability, and ϖ is defined by the dispersion relation

$$\varpi^2 - \boldsymbol{B}\cdot\boldsymbol{k}/(\rho\mu) = \pm\varpi(2\boldsymbol{\Omega}\cdot\boldsymbol{k}/k). \tag{40}$$

Thus, for both waves, we can write $\hat{\boldsymbol{\omega}} = \mp k'\hat{\boldsymbol{u}}$, where k' is an effective wave number. Once again, if the steps in Sec. III are followed, a superposition of these waves is also likely to result in a similar pattern of helicity segregation that is observed for a monochromatic inertial wave. Moreover, if the magnetic diffusion (also called Ohmic dissipation) is included in the governing equations, we can see that once again it only dampens the wave amplitudes without affecting their helical structure. These observations agree with those in geodynamo simulations in the presence of strong magnetic field [Fig. 1(a) [10] for example] wherein there is a clear segregation of helicity. As the magnetic field in the core is not uniform, the low-frequency inertial wave packets which are triggered near the equator may be damped before they reach the mantle, depending on the rotation versus damping time scales. Perhaps, they could be transformed into hybrid magnetic-inertial waves which also retain the helicity segregation characteristic of inertial waves [25,26].

3. Buoyancy

In several geophysical settings, such as in the atmosphere and the oceans, the buoyancy force is also important apart from the Coriolis force. Often, a stable stratification is present which supports internal gravity waves [27] that are analogous to inertial waves in rotating fluids [28]. Even in the core, the outermost part is reported to be stably stratified [29]. To study such a flow, let us now consider the governing equations in the rotating frame with the Boussinesq approximation (small density perturbations)

$$\frac{\partial\boldsymbol{u}}{\partial t} = -\frac{1}{\rho}\nabla\tilde{p} - 2\boldsymbol{\Omega}\times\boldsymbol{u} + c\boldsymbol{g}, \tag{41}$$

$$\frac{\partial c}{\partial t} = \frac{N^2}{g}u_z, \tag{42}$$

where $c = \rho'/\rho$, ρ' is the density perturbation, $\boldsymbol{g} = -g\hat{\boldsymbol{e}}_z$, and $N = [-(g/\rho)(d\rho_0/dz)]^{1/2}$ is the buoyancy frequency. The vorticity equation, therefore, is

$$\frac{\partial\boldsymbol{\omega}}{\partial t} = 2(\boldsymbol{\Omega}\cdot\nabla)\boldsymbol{u} + \nabla c\times\boldsymbol{g}. \tag{43}$$

Let us now find the helicity of a monochromatic inertia-gravity wave, the analog of inertial waves in a rotating-stratified system. Assume $c = \hat{c}\exp[i(\boldsymbol{k}\cdot\boldsymbol{x} - \varpi t + \phi)]$, where ϕ is the phase difference with the velocity and vorticity wave vectors which vary according to the form (5). Using (42), we find

$$c = \frac{iN^2\hat{u}_x}{g\varpi}\exp[i(\boldsymbol{k}\cdot\boldsymbol{x} - \varpi t)], \tag{44}$$

which implies $\phi = \pi/2$, and $\hat{c} = N^2\hat{u}_x/g\varpi$. We can, therefore, write

$$\nabla c\times\boldsymbol{g} = icg(k_x\hat{\boldsymbol{e}}_y - k_y\hat{\boldsymbol{e}}_x). \tag{45}$$

Using (45) and (43), we can write the vorticity amplitudes as

$$\begin{aligned}\hat{\omega}_x &= -\frac{2\Omega k_z}{\varpi}\hat{u}_x + i\frac{N^2 k_y}{\varpi^2}\hat{u}_z,\\ \hat{\omega}_y &= -\frac{2\Omega k_z}{\varpi}\hat{u}_y - i\frac{N^2 k_x}{\varpi^2}\hat{u}_z,\\ \hat{\omega}_z &= -\frac{2\Omega k_z}{\varpi}\hat{u}_z,\end{aligned} \tag{46}$$

where ϖ is now defined by the dispersion relation

$$\varpi^2 = 4\Omega^2\frac{k_z^2}{k^2} + N^2\frac{k_x^2 + k_y^2}{k^2}. \tag{47}$$

Note that these reduce to the corresponding relationships for inertial waves when $N = 0$. The polarization relations for these waves can be found using (26) and the dispersion relation. The helicity of a monochromatic wave can, therefore, be obtained:

$$h = -\frac{2\Omega k_z}{\varpi}(\mathrm{Re}[u_x]^2 + \mathrm{Re}[u_y]^2 + \mathrm{Re}[u_z]^2) - \frac{N^2}{\varpi^2}(k_y\mathrm{Re}[u_x] - k_x\mathrm{Re}[u_y])\mathrm{Im}[u_z]. \tag{48}$$

The first term is reminiscent of the helicity of inertial waves, but does not equal $\mp k|\hat{\boldsymbol{u}}|^2$ as the frequency is now defined by (47). When rotation is absent, the helicity is zero (as would be expected for internal gravity waves) since $\hat{\omega}_z = i(k_x\hat{u}_y - k_y\hat{u}_x) = 0$ from (46). Moreover, this estimate for helicity suggests that for a monochromatic inertia-gravity wave, the segregation now depends not only on the values of k_x,k_y,k_z but also on the strength of stratification relative to rotation ($N/2\Omega$). Thus, inertia-gravity waves traveling along $+z$ could have both positive or negative helicity. Similar amplitude and helicity relationships can be obtained and similar observations can be made for the cases when the direction of gravity is not parallel to rotation, as is the case in the core. Recently, Duarte *et al.* [30] found an inverted sign of (azimuthally averaged) helicity, i.e., positive in the north and negative in the south, in their solar dynamo simulations with mild stratification in the interior. The "inversion mechanism" proposed by them relies on the generation of positive radial vorticity in upwelling flows due to the action of the density gradient and the Coriolis force. This can be understood if we consider a quasisteady version of Eq. (43), $\partial\boldsymbol{\omega}/\partial t \approx 0$, in which a balance exists between the Coriolis and the buoyancy terms. However, in a dynamic system, the inertia-gravity waves, which are essentially oscillations about the equilibrium, and wave packets could play an important role in the helicity inversion.

Of course, if $N = 0$ there are no inertia-gravity waves but there can still be a "local" generation of helicity through vorticity (43). To see how, consider the evolution equation for helicity which can be derived using (41) and (43):

$$\frac{\partial h}{\partial t} = -\frac{1}{\rho}(\boldsymbol{\omega}\cdot\nabla\tilde{p}) - 2\boldsymbol{\omega}\cdot(\boldsymbol{\Omega}\times\boldsymbol{u}) + 2\boldsymbol{u}\cdot(\boldsymbol{\Omega}\cdot\nabla)\boldsymbol{u} + \boldsymbol{\omega}\cdot c\boldsymbol{g} + \boldsymbol{u}\cdot\nabla c\times\boldsymbol{g}. \tag{49}$$

Using appropriate vector identities and zero divergence of velocity and vorticity, the first three terms on the right-hand side can be combined as $\nabla\cdot[-(\boldsymbol{\omega}\tilde{p}/\rho) + 2(\boldsymbol{u}\cdot\boldsymbol{\Omega})\boldsymbol{u})]$. Under geostrophic balance, the divergence of these terms should be zero, so that the other terms represent the ageostrophic helicity sources due to the combined action of buoyancy and rotation, which can be computed in numerical simulations. Indeed, both positive and negative helicity can be created by the buoyancy field as was observed by Davidson and Ranjan [4] [see Fig. 1(c)].

4. Nonlinearity

The discussion below is about the nonlinearity due to the advection term in Eq. (1) which is often called the "inertial term," a nomenclature that we avoid so as to prevent confusion with *inertial*

waves. So far in this study, we have considered the linear limit when the Coriolis forces dominate, i.e., when the Ro $\ll 1$. Recent studies have shown that inertial waves dominate the dynamics up to Ro $= 0.4$ both in the context of rotating turbulence [31] and for geophysical vortices [32]. However, in the regime $0.4 <$ Ro < 1, when both Coriolis and nonlinear terms may be important, inertial waves may not only exist but may even interact nonlinearly. Note that this (strong) interaction is different from the weakly nonlinear resonant-triad interactions [33,34] in the low Ro $\ll 1$ but high Re limit. Using numerical simulations, Zhang, Yi, and Wang [35] investigated the nonlinear evolution of an internal gravity wave packet and found that the temporal variation of the amplitudes and phases was as would be expected according to the linear gravity theory. If we speculate that this would also apply to inertial waves, we might then ask whether the inertial wave packets retain their helicity characteristic when they interact. According to Kraichnan [36], for a wave triad such that their wave numbers are related as $\boldsymbol{k} = \boldsymbol{p} + \boldsymbol{q}$, the wave $\boldsymbol{k}$ does not necessarily have the helicity of the same sign as that of the other two waves $\boldsymbol{p}$,$\boldsymbol{q}$ which are of maximal helicity. This observation agrees well with the experiments of Bordes *et al.* [34] where the helicity of the two secondary waves arising due to subharmonic instability was neither maximal nor was it necessarily of the same sign as that of the primary inertial wave with maximal helicity. Thus, it is possible that several such (nonlinear) interactions between inertial waves may indeed lead to the production of helicity of opposite sign. A similar behavior might be expected if the waves exist along with a significant mean flow [37]. However, since the Ro in the core is believed to be rather small [12] ($\sim 10^{-6}$), the nonlinear term in the momentum equation is unlikely to be important.

B. Presence of boundaries

In many geophysical situations such as the core, the presence of a physical boundary can affect the helicity of inertial waves. Incorporating the correct boundary conditions leads to normal-mode solutions of the wave equation (4) which have been described at length by Greenspan [14]. These are inertial *modes* which share some characteristics with their unbounded twin—the inertial waves, such as the dispersion relation, the range of frequency $[-2\Omega, 2\Omega]$—and have even been detected in the core [38]. But are the monochromatic inertial modes maximally helical? Not necessarily. This is because on reflection from the boundary, the sign of helicity reverses since the frequency $(2\boldsymbol{\Omega} \cdot \boldsymbol{k}/k)$ and the sense of rotation are conserved [39]. To illustrate this quantitatively, if we consider the solutions of the boundary-value problem obtained for a rotating cylindrical annulus by Zhang *et al.* [15] and calculate the helicity of a monochromatic inertial mode, we will find that its sign can be both positive or negative for $\pm z$ (see details in the Appendix). One may speculate that this argument can be extended to inertial modes in a spherical shell [15] and also to those modes that are excited by thermal instabilities [16]. Moreover, although the inertial mode is not a (stationary) standing wave [14], their frequency is determined by the boundary unlike that in the case of waves where it is mostly determined by the initial wave-number distribution of the fluid disturbance. Since the helicity of inertial waves could be an important ingredient for the α^2 geodynamo model [5], perhaps it is wise to distinguish the modes from the waves, particularly in the context of an enormous and vigorously convective system such as the core where both may coexist. This distinction will also apply to the family of Rossby waves [22] which can exist in confined systems and are reported to be special type of low-frequency inertial modes [14].

VI. CONCLUSIONS

In this study, we have investigated the helicity of inertial wave packets formed by linear superposition of monochromatic waves propagating in a particular direction. For this purpose, we first derive a general form of the polarization relations for inertial waves (22). We find that the helicity of an inertial wave packet is likely to possess the segregation characteristic (negative above and positive below) of monochromatic waves unless the wave-number magnitudes are widely separated in which case helicity of the opposite sign may result. This has been illustrated using a

linear superposition of four monochromatic inertial waves. The DNS of a Gaussian eddy under rapid rotation reveals that for slowly modulated wave packets the segregation characteristic is likely to hold. This segregation is also seen in several geodynamo simulations and is an important ingredient in the α^2-dynamo models, particularly in the model based on inertial waves [5]. Furthermore, the polarization relations derived in this study can be used to estimate other interesting quantities such as the kinetic energy transport, wave action, and the wave-induced mean flow for inertial waves, as has already been done for internal gravity waves [27].

We also discuss the change (if any) in this segregation characteristic due to the dissipative, Lorentz, buoyancy, and nonlinear forces. The helical structure of the wave packet is likely to be unchanged in the presence of the Lorentz force or viscous dissipation [8]. However, a dominance of (stable) stratification is likely to modify this characteristic and so is the presence of nonlinearity. To be more conclusive, these findings need to be tested using model problems such as a Gaussian eddy or a buoyant blob for different (relative) strengths of the dominant forces. In the core, the Coriolis and the Lorentz force are said to be the most important forces. This indicates that the dynamics in the core could support weakly modified inertial waves and hybrid magnetic-inertial waves [25,26] which retain their helicity segregation characteristic in the presence of the magnetic field. However, there could be other local sources of helicity apart from the waves which may be present in the core, such as the Ekman layers or localized buoyancy sources. Work is underway to test these ideas using model problems and spherical geodynamo simulations. Lastly, the results derived in this study for inertial wave packets can be readily extended to magnetostrophic wave packets and used for computing the total helicity estimates equivalent to (32) for the cross helicity ($\boldsymbol{u}\cdot\boldsymbol{B}$) or the magnetic helicity [6] ($\boldsymbol{A}\cdot\boldsymbol{B}$, where $\nabla\times\boldsymbol{A}=\boldsymbol{B}$).

ACKNOWLEDGMENT

The author wishes to thank Professor P. Davidson for useful comments, Professor P. K. Yeung for his pseudospectral DNS code, the Leverhulme Trust, UK, for the research fellowship, and the reviewers for their suggestions.

APPENDIX

Here we calculate the helicity of inertial modes. Following are the velocity solutions of the boundary-value problem in a rotating cylindrical annulus which were obtained by Zhang *et al.* [15] (see Appendix of his paper). We follow his notation, so that $\sigma=\varpi/2\Omega$ where $|\sigma|<1$. The velocity components of inertial modes in cylindrical coordinates (s,ϕ,z) are

$$\begin{aligned} u_s &= -i\left(\sigma f'(s)+\frac{mf(s)}{s}\right)\cos(n\pi z)\exp i(m\phi+2\sigma t),\\ u_\phi &= \left(f'(s)+\frac{m\sigma f(s)}{s}\right)\cos(n\pi z)\exp i(m\phi+2\sigma t),\\ u_z &= -i\frac{(1-\sigma^2)}{\sigma}n\pi f(s)\sin(n\pi z)\exp i(m\phi+2\sigma t), \end{aligned} \tag{A1}$$

where m is the azimuthal wave number, n is the number of zeros along z, the superscript $'$ denotes the derivative with respect to s, and

$$\begin{aligned} f(s) = {}& [m(1-\sigma)^{1/2}K_m(\xi_o)+n\pi s_o(1+\sigma)^{1/2}K_{m-1}(\xi_o)]J_m(\xi)\\ & -[m(1-\sigma)^{1/2}J_m(\xi_o)+n\pi s_o(1+\sigma)^{1/2}J_{m-1}(\xi_o)]K_m(\xi) \end{aligned} \tag{A2}$$

so that the subscript "o" denotes the outer radius of the cylinder,

$$\xi=\frac{n\pi}{\sigma}(1-\sigma^2)^{1/2},$$

and J_m, K_m are the Bessel functions of the first and second kind, respectively. The helicity of the mode can be written as

$$h = u_s\omega_s + u_\phi\omega_\phi + u_z\omega_z, \tag{A3}$$

where

$$\begin{aligned}\omega_s &= \left(\frac{1}{s}\frac{\partial u_z}{\partial \phi} - \frac{\partial u_\phi}{\partial z}\right),\\ \omega_\phi &= \left(\frac{\partial u_s}{\partial z} - \frac{\partial u_z}{\partial s}\right),\\ \omega_z &= \frac{1}{s}\left(\frac{\partial s u_\phi}{\partial s} - \frac{\partial u_s}{\partial \phi}\right).\end{aligned} \tag{A4}$$

After some algebra, we find the vorticity components and helicity to be

$$\begin{aligned}\omega_s &= \left(\frac{mf(s)}{s\sigma} + f'(s)\right)(n\pi)\sin(n\pi z)\exp i(m\phi + 2\sigma t),\\ \omega_\phi &= i\left(\frac{mf(s)}{s} + \frac{f'(s)}{\sigma}\right)(n\pi)\sin(n\pi z)\exp i(m\phi + 2\sigma t),\\ \omega_z &= \left(f''(s) + \frac{f'(s)}{s} - \frac{m^2 f(s)}{s^2}\right)\cos(n\pi z)\exp i(m\phi + 2\sigma t),\end{aligned} \tag{A5}$$

$$h = iH\exp i(m\phi + 2\sigma t), \tag{A6}$$

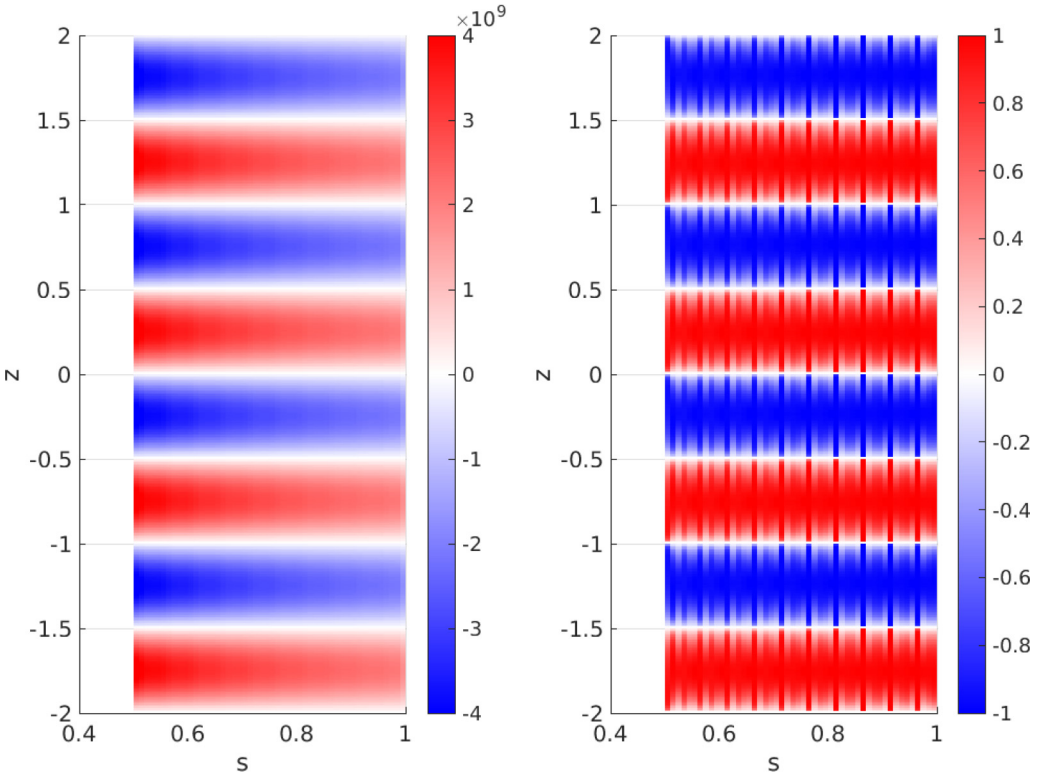

FIG. 5. H (left) and h_r (right) for inertial modes in a cylindrical annulus.

where

$$H = \left([f'(s)]^2 - f(s)f''(s) - \frac{f(s)f'(s)}{s} \right) \left(\frac{1}{\sigma} - \sigma \right) \frac{(n\pi)\sin(2n\pi z)}{2}$$

and the superscript $''$ denotes the second derivative with respect to s. The relative helicity can be calculated as $h_r = h/|\boldsymbol{u}||\boldsymbol{\omega}|$. For illustration, we choose $m = 5$, $n = 1$, $\sigma = 0.05$, for a cylindrical annulus in which $0.5 < s < 1.0$ and $-2.0 < z < 2.0$. The plots of H and h_r are shown in Fig. 5. It is evident that the helicity sign of the inertial modes changes sinusoidally in z so that the modes vary from being maximally helical to nonhelical for both positive and negative z. However, the modes are close to being maximally helical in the s direction. This holds for other values of m,n,σ as well, not shown here. This result is not surprising given that the velocity and vorticity amplitudes in s,ϕ are aligned whereas those in z are not.

[1] H. K. Moffatt, The degree of knottedness of tangled vortex lines, J. Fluid Mech. **35**, 117 (1969).

[2] H. K. Moffatt, Dynamo action associated with random inertial waves in a rotating conducting fluid, J. Fluid Mech. **44**, 705 (1970).

[3] A. Ranjan and P. A. Davidson, Evolution of a turbulent cloud under rotation, J. Fluid Mech. **756**, 488 (2014).

[4] P. A. Davidson and A. Ranjan, Planetary dynamos driven by helical waves-ii, Geophys. J. Int. **202**, 1646 (2015).

[5] P. A. Davidson, The dynamics and scaling laws of planetary dynamos driven by inertial waves, Geophys. J. Int. **198**, 1832 (2014).

[6] H. K. Moffatt, Helicity and celestial magnetism, Proc. R. Soc. London, Ser. A **472**, 20160183 (2016).

[7] E. N. Parker, Hydromagnetic dynamo models, Astrophys. J., Lett. **122**, 293 (1955).

[8] H. K. Moffatt, *Magnetic Field Generation in Electrically Conducting Fluids* (Cambridge University Press, Cambridge, England, 1978).

[9] P. Olson, U. Christensen, and G. A. Glatzmaier, Numerical modeling of the geodynamo: mechanisms of field generation and equilibration, J. Geophys. Res. **104**, 10383 (1999).

[10] B. Sreenivasan, S. Sahoo, and G. Dhama, The role of buoyancy in polarity reversals of the geodynamo, Geophys. J. Int. **199**, 1698 (2014).

[11] A. Sakuraba and P. H. Roberts, Generation of a strong magnetic field using uniform heat flux at the surface of the core, Nat. Geosci. **2**, 802 (2009).

[12] P. A. Davidson, *Turbulence in Rotating, Stratified and Electrically Conducting Fluids* (Cambridge University Press, Cambridge, England, 2013).

[13] P. A. Davidson, P. J. Staplehurst, and S. B. Dalziel, On the evolution of eddies in a rapidly rotating system, J. Fluid Mech. **557**, 135 (2006).

[14] H. P. Greenspan, *The Theory of Rotating Fluids* (Cambridge University Press, Cambridge, England, 1968).

[15] K. Zhang, P. Earnshaw, X. Liao, and F. H. Busse, On inertial waves in a rotating fluid sphere, J. Fluid Mech. **437**, 103 (2001).

[16] K. Zhang, X. Liao, and D. Kong, Inertial convection in a rotating narrow annulus: Asymptotic theory and numerical simulation, Phys. Fluids **27**, 106604 (2015).

[17] L. Messio, C. Morize, M. Rabaud, and F. Moisy, Experimental observation using particle image velocimetry of inertial waves in a rotating fluid, Exp. Fluids **44**, 519 (2008).

[18] S. Chandrasekhar, *Hydrodynamic and Hydromagnetic Stability* (Clarendon, Oxford, 1961).

[19] E. Yarom and E. Sharon, Experimental observation of steady inertial wave turbulence in deep rotating flows, Nat. Phys. **10**, 510 (2014).

[20] P. K. Yeung and Y. Zhou, Numerical study of rotating turbulence with external forcing, Phys. Fluids **10**, 2895 (1998).

[21] R. S. Rogallo, Numerical experiments in homogeneous turbulence, Technical Report No. 81835, NASA Tech. Mem. 1981.
[22] C. C. Finlay, Waves in the presence of magnetic fields, rotation and convection, Dynamos Les Houches Session **88**, 403 (2008).
[23] A. Tilgner, Oscillatory shear layers in source driven flows in an unbounded rotating fluid, Phys. Fluids **12**, 1101 (2000).
[24] B. Lehnert, Magnetohydrodynamic waves under the action of the coriolis force, Astrophys. J., Lett. **119**, 647 (1954).
[25] O. Bardsley and P. Davidson, Inertial–alfvén waves as columnar helices in planetary cores, J. Fluid Mech. **805**, R2 (2016).
[26] O. Bardsley and P. Davidson, The dispersion of magnetic-coriolis waves in planetary cores (unpublished).
[27] B. R. Sutherland, *Internal Gravity Waves* (Cambridge University Press, Cambridge, England, 2010).
[28] G. Veronis, The analogy between rotating and stratified fluids, Annu. Rev. Fluid Mech. **2**, 37 (1970).
[29] B. Buffett, N. Knezek, and R. Holme, Evidence for mac waves at the top of earth's core and implications for variations in length of day, Geophys. J Int. **204**, 1789 (2016).
[30] L. Duarte, J. Wicht, M. K. Browning, and T. Gastine, Helicity inversion in spherical convection as a means for equatorward dynamo wave propagation, Mon. Not. R. Astron. Soc. **456**, 1708 (2016).
[31] Y. B. Baqui, P. A. Davidson, and A. Ranjan, Are there two regimes in strongly rotating turbulence? Phys. Fluids **28**, 045103 (2016).
[32] P. Wang and T. M. Özgökmen, Spiral inertial waves emitted from geophysical vortices, Ocean Modell. **99**, 22 (2016).
[33] L. M. Smith and F. Waleffe, Transfer of energy to two-dimensional large scales in forced, rotating three-dimensional turbulence, Phys. Fluids **11**, 1608 (1999).
[34] G. Bordes, F. Moisy, T. Dauxois, and P. Cortet, Experimental evidence of a triadic resonance of plane inertial waves in a rotating fluid, Phys. Fluids **24**, 014105 (2012).
[35] S. Zhang, F. Yi, and J. Wang, The nonlinear effects on the characteristics of gravity wave packets: dispersion and polarization relations, Ann. Geophys. **18**, 1316 (2000).
[36] R. H. Kraichnan, Helical turbulence and absolute equilibrium, J. Fluid Mech. **59**, 745 (1973).
[37] A. Campagne, B. Gallet, F. Moisy, and P.-P. Cortet, Disentangling inertial waves from eddy turbulence in a forced rotating-turbulence experiment, Phys. Rev. E **91**, 043016 (2015).
[38] K. D. Aldridge and L. I. Lumb, Inertial waves identified in the earth's fluid outer core, Nature (London) **325**, 421 (1987).
[39] O. M. Phillips, Energy transfer in rotating fluids by reflection of inertial waves, Phys. Fluids **6**, 513 (1963).